

Universal Defect Statistics in Counterdiabatic Quantum Critical Dynamics

Andras Grabarits^{1,*} and Adolfo del Campo^{1,2}

¹*Department of Physics and Materials Science, University of Luxembourg, L-1511 Luxembourg, Luxembourg*

²*Donostia International Physics Center, E-20018 San Sebastian, Spain*

Counterdiabatic driving (CD) provides a framework to reduce excitations in nonadiabatic processes. Exact CD protocols require nonlocal control fields, and CD approximations with tailored locality are needed for their implementation. However, the performance of local CD schemes remains poorly understood. We consider the local CD across a quantum phase transition at an arbitrary rate. We establish its efficiency as a function of the degree of locality and demonstrate that the resulting defect statistics exhibit universal behavior. Our results provide an analytical framework for evaluating the effectiveness of local CD protocols in quantum state preparation, control, and optimization.

Adiabatic protocols play a key role in quantum control, but their implementation generally requires slow driving. In certain scenarios, they are thus not applicable. This is the case when driving a continuous quantum phase transition (QPT), characterized by the closing of the gap between the ground and the first excited state at the critical point. Across a QPT, adiabaticity breaks down, giving rise to defects as excitations [1–3]. Yet, the adiabatic crossing of QPTs at a finite driving rate is desirable for a range of important applications, such as quantum state preparation in quantum simulation and adiabatic quantum computation [4, 5]. A variety of approaches have been investigated for defect suppression. They involve quantum control [6, 7], nonlinear driving [8, 9], inhomogeneous or local driving [10–12], multi-parameter driving [13], a symmetry-breaking bias [14, 15], and coupling to a tailored environment [16–19]. Defect suppression is also enhanced in specific scenarios that involve the crossing of gapless lines and multicritical points [20, 21] and broken chiral symmetry [22].

A powerful and versatile approach relies on assisting the time evolution with additional control fields for counterdiabatic driving (CD) [23–26]. The auxiliary CD fields are highly nonlocal in many-body systems, making their experimental implementation in quantum devices challenging [27–29]. This motivates the search for approximate CD schemes with controlled locality to ease their implementation. Local CD protocols can be designed using variational methods [30, 31] and truncated expansions in Krylov space [32–34]. The combination of approximate CD controls with digital quantum simulation paves the way for their implementation. Defect suppression across a QPT has recently been demonstrated by Trotterizing the dynamics in the circuit model for quantum computation [35]. Yet, while the performance of exact CD protocols with nonlocal control fields is identical to that of adiabatic driving and leads to a complete defect suppression, the performance of approximate CD remains poorly understood.

In this Letter, we provide an exact characterization of the defect statistics upon crossing a QPT when the dynamics is assisted by approximate CD. In particular, we

analyze approximate CD schemes with tunable locality resulting from the CD expansion at a given order in the transverse-field Ising model (TFIM) and show that our predictions hold universally in general critical systems.

Defect statistics in the transverse field Ising model. The TFIM provides an ideal testbed to study the fundamental analytical properties of QPTs [1, 36–38]. It is described by the interacting spin Hamiltonian given by

$$\hat{H}(t) = -J \sum_{j=1}^L (\hat{\sigma}_j^z \hat{\sigma}_{j+1}^z + g(t) \hat{\sigma}_j^x), \quad (1)$$

with ferromagnetic couplings, fixed as $J = 1$ for convenience. We consider a linear protocol $g = g(0)(1 - t/T)$ during the interval $t \in [0, T]$, starting deep in the paramagnetic phase (e.g., $g(0) = 100$), and terminating in the ferromagnetic phase, $g(T) = 0$. Mapping (1) to independent two-level systems (TLSs) by a Jordan-Wigner transformation and a subsequent Fourier decomposition [38] yields $\hat{H} = 2 \sum_{k>0} \hat{\phi}_k^\dagger [(g(t) - \cos k)\tau^z + \sin k \tau^x] \hat{\phi}_k = 2 \sum_{k>0} \hat{\phi}_k^\dagger H_k(t) \hat{\phi}_k$, with $\hat{\phi}_k = (c_k^\dagger, c_{-k})^T$ containing the fermionic creation and annihilation operators of each mode labeled by the momentum $k = \pm \frac{\pi}{L}, \pm \frac{3\pi}{L}, \dots, \pm \pi \mp \frac{\pi}{L}$. Simultaneous excitations in these modes, $(-k, k)$, correspond to topological defects that translate to kink pairs due to the \mathbb{Z}_2 -symmetry of the ferromagnetic ground state.

The number of kinks can be captured by the expectation value of the kink number operator, $\hat{N} = \frac{1}{2} \sum_{j=1}^L (1 - \hat{\sigma}_j^z \hat{\sigma}_{j+1}^z)$ as $\langle N(T) \rangle = \langle \Psi(T) | \hat{N} | \Psi(T) \rangle = 2 \sum_{k>0} \langle \gamma_k^\dagger(T) \gamma_k(T) \rangle$. The second expression counts the number of excitations in the TLSs via the Bogoliubov operators diagonalizing $\hat{\psi}_k^\dagger H_k(T) \hat{\psi}_k$ at time T . For slow annealing schedules, the excitation probabilities are precisely captured by the Landau-Zener (LZ) transition probability given by $p_k = \langle \gamma_k^\dagger(T) \gamma_k(T) \rangle \approx e^{-2\pi k^2 T}$, leading to $\langle N(T) \rangle = 2 \sum_{k>0} p_k \approx (8\pi^2 T)^{-1/2} L$ [37, 39, 40]. This result agrees with the original argument of the Kibble-Zurek mechanism (KZ), which predicts $\langle N(T) \rangle \sim T^{-d\nu/(1+z\nu)} L$ in d dimensions for point-like defects [41–45], with $z = \nu = 1$ in $d = 1$ dimension. For fast

quenches, there is a universal breakdown of the KZ scaling [46, 47] for time scales of $T_{\text{fast}} \sim O(1)$. In the limit of sudden quenches, $p_k = \cos^2(k/2) + \mathcal{O}(T^{1/2})$ for all k , leading to saturation of $\langle N(T) \rangle \approx 1/2$.

Beyond the average defect number, the complete statistical characterization is given by the kink distribution $P(N; T) = \langle \Psi(T) | \delta(\hat{N} - N) | \Psi(T) \rangle$ [48]. As shown in Ref. [49–51], the kink pair statistics in the TFIM is given by a Poisson-binomial distribution, as verified in various experimental platforms [50, 52–54]. The characteristic function is related to $P(N; T)$ by a Fourier transform, $\tilde{P}(\theta; T) = \mathbb{E}[e^{i\theta N}]$. Its logarithm, the cumulant generating function, $\log \tilde{P}(\theta; T) = \log \mathbb{E}[e^{i\theta N}] = \sum_{q=1}^{\infty} (i\theta)^q \frac{\kappa_q}{q!}$, offers an elegant way to characterize the defect statistics in terms of cumulants, defined as $\kappa_q(T) = (i\partial_\theta)^q \log \tilde{P}(\theta; T) \Big|_{\theta=0}$. In the TFIM, $\log \tilde{P}(\theta; T)$ simplifies to the sum of cumulant generating functions of the TLSs, which are given by Bernoulli random variables with p_k [48], $\log \tilde{P}(\theta; T) = \sum_{k>0} \log [1 + (e^{2i\theta} - 1) p_k]$. In the limit of slow annealing schedules, it was shown theoretically and verified in a wide range of experiments that all cumulants follow the same power law of T and are thus proportional to the mean, $\kappa_q(T) \propto \kappa_1(T) = \langle N(T) \rangle$. On the other hand, in the fast quench regime, all the cumulants can be expressed in a closed form as $\kappa_q(T \rightarrow 0) = \frac{L}{4} \frac{2^{2q} - 1}{2^{2q} - 1} B_{2q} + O(T^{1/2})$ with B_{2q} denoting the $2q$ -th Bernoulli number [47].

Counterdiabatic driving. Consider the adiabatic trajectory generated by an uncontrolled system Hamiltonian $H[g(t)]$. CD makes it possible to fast-forward such evolution at an arbitrary rate by assisting the dynamics with the (exact) CD term so that the total Hamiltonian reads [23–26], $H_{\text{CD}}(t) = H[g(t)] + \dot{g} \cdot H_1[g(t)]$, where $H_1[g] = i \sum_n (|d_g n\rangle \langle n| - |n\rangle \langle n| d_g) |n\rangle \langle n|$. This Hamiltonian becomes highly non-local in many-body systems, in particular across a QPT, making its experimental implementation challenging [27, 30]. To address this issue, a feasible strategy is provided by the nested-commutator expansion with a controlled locality [32], which is most efficiently obtained within the Krylov subspace. As shown in Ref. [27, 29, 33], the k -th term in the Krylov expansion in the TFIM of the exact CD Hamiltonian is given by

$$H_1 = -\dot{g}(t) \sum_{l=1}^{L/2} \frac{2}{L+2} \sum_{j=1}^{L/2} \frac{\sin\left(\frac{\pi j}{L/2+1}\right) \sin\left(\frac{l\pi j}{L/2+1}\right)}{1+g^2-2g \cos\left(\frac{\pi j}{L/2+1}\right)} \\ \times \sum_{k>0} \sin(lk) \hat{\varphi}_k^\dagger \tau_k^y \hat{\varphi}_k \equiv \sum_{k>0} q_k(t) \hat{\varphi}_k^\dagger \tau_k^y \hat{\varphi}_k. \quad (2)$$

Here, $q_k(t)$ was introduced for the exact CD term in the k -th TLS. The Krylov expansion of $q_k(t)$ up to order n reads $q_k^{(n)}(T) = -\dot{g} \sum_{m=1}^n \frac{\sin(km) g^{2m} (1+g^L)}{2 g^{m+1} + g^L}$ [29].

Exact fast-quench kink statistics and adiabatic limit. Near the sudden limit, $T \rightarrow 0$, the number of kinks saturates at a plateau that becomes independent of

the driving time T . The effect of $H_k(t)$ can be neglected in this limit. However, the CD term preserves the finite rate evolution form as it is proportional to the speed of the quench $\dot{g} \sim 1/T$. Thus, the time-dependent Schrödinger equation is governed solely by the off-diagonal element, $\partial_t [\psi_{k,1}(t), \psi_{k,2}(t)]^T = -i q_k^{(n)}(t) \tau^y [\psi_{k,1}(t), \psi_{k,2}(t)]^T$ for the k -th TLS. As the time dependence only appears via the multiplicative factor, the result can readily be obtained by acting with the operator $e^{-i \int_0^T dt' q_k^{(n)}(t') \tau^y}$ on the initial state $(0, 1)^T$, leading to $[\psi_{k,1}(T), \psi_{k,2}(T)]^T = [-\sin[\text{Si}(n, k)], \cos[\text{Si}(n, k)]]^T$, where we have defined $\text{Si}(n, k) = \sum_{m=1}^n \frac{\sin(km)}{m}$, as detailed in [55]. As a result, the excitation probability of mode k under the approximate local CD of order n can be expressed in closed form,

$$p_k^{(n)} = \sin^2 \frac{k}{2} \sin^2 [\text{Si}(n, k)] + \cos^2 \frac{k}{2} \cos^2 [\text{Si}(n, k)] \\ - \frac{1}{2} \sin k \sin [2\text{Si}(n, k)], \quad (3)$$

whose high accuracy is demonstrated in [55]. This formula makes it possible to characterize the kink number distribution and its cumulants with a low-order CD expansion. Remarkably, even the first-order term in the CD expansion changes completely the fast quench cumulants, $\kappa_1^{(1)}(0) \approx 0.2L$, $\kappa_2^{(1)}(0) \approx 0.096L$, $\kappa_3^{(1)}(0) \approx 0.112L$, compared to those without CD, $\kappa_1(0) = 1/2$, $\kappa_2(0) = 1/4$, $\kappa_3(0) = 0$. In addition, it leads to finite skewness corrections in the defect statistics.

Surprisingly, even for a low number of CD terms, $n \gtrsim \sqrt{L}/10$, the excitation probabilities and the kink statistics can be precisely captured by the analytical results of the large-order expansion limit $n \sim \sqrt{L}$. As shown in [55], the excitation probabilities admit a remarkably compact limiting form given by

$$p_k^{(n)} \approx \cos^2 [\text{Si}(nk)], \quad (4)$$

where the sine integral has been introduced, $\text{Si}(z) = \int_0^z dx \frac{\sin x}{x}$. Note that the CD order only appears as a simple scaling factor of the momentum. As a result, the cumulant generating function in the sudden limit acquires a universal dependence on n ,

$$\log \tilde{P}^{(n)}(\theta; 0) \approx \frac{1}{n} \int_0^\infty dx \log \{1 + (e^{2i\theta} - 1) \cos^2 [\text{Si}(x)]\}. \quad (5)$$

It thus follows that all cumulants of the kink number distribution are inversely proportional to n ,

$$\kappa_q^{(n)}(0) \propto 1/n. \quad (6)$$

The average and the variance are $\kappa_1^{(n)}(0) \approx 1.05/\pi L n^{-1}$ and $\kappa_2^{(n)}(0) \approx 0.86/\pi L n^{-1}$, with the ratio $\kappa_2^{(n)}(0)/\kappa_1^{(n)}(0) \approx 0.82$, implying sub-Poissonian

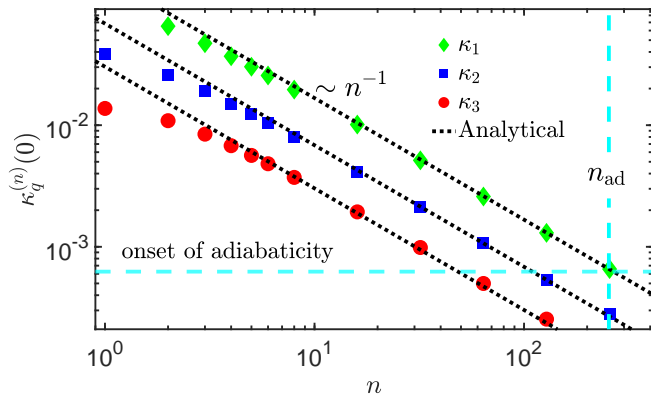


FIG. 1. Universal scaling of the first three cumulants – characterizing the mean, variance, and third centered moment of the distribution – in the fast quench regime as a function of the CD order. The analytically obtained constant prefactors provide a precise slope ($L = 1600$ and $T = 1$).

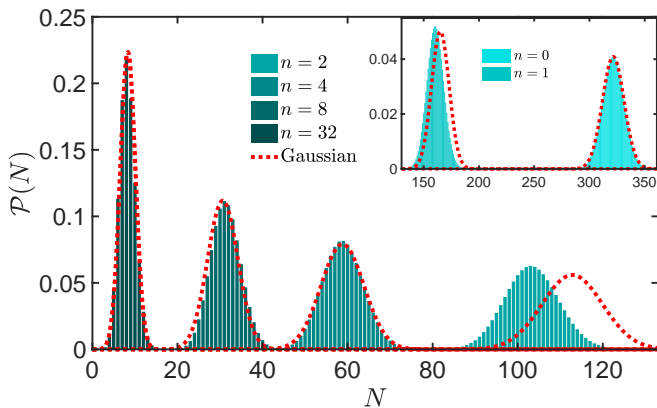


FIG. 2. Kink statistics in the fast quench regime for considerably away from the sudden limit, $T = 2$ for various CD expansion orders, displaying remarkable agreement with the Gaussian distributions of the average and variance obtained by large order analytical results. As the CD order is increased, defect suppression manifests in the gradual shift of the distributions towards zero with decreasing width. Inset shows the defect statistics without CD and for $n = 1$ with the exact low-order results of Eq. (4) ($L = 1600$, $T = 2$).

statistics with a distinct behavior from the KZ scaling regime without CD [49, 52]. The third cumulant is given by $\kappa_3^{(n)}(0) \approx 0.76/\pi L n^{-1}$ implying sub-Poissonian skewness corrections, $\kappa_3^{(n)}(0)/\kappa_1^{(n)}(0) \approx 0.73$ on the right side of the distributions as the Gaussian limit is reached. The numerical verification of the CD order scaling of the first three cumulants is demonstrated in Fig. 1. Additional plots in the SM. [55]) illustrate the crossover from the constant plateau values of the cumulant ratio in the fast quench to those of the slow driving limit.

We also demonstrate the effect of the local expansion of

CD on defect statistics. As the excitation of each mode is described by an independent Bernoulli random variable, the defect distribution can be approximated as a normal distribution, characterized solely by the first two cumulants. In agreement with the cumulant scaling as n increases, both the center of the distributions and their width converge to zero, as demonstrated in Fig. 2. Remarkably, even for $n = 2$ precise matching is given with the large order form of p_k^2 , Eq. (4), while the inset of Fig. 2 clearly shows that similar errors are present with the exact form of $p_k^{(n)}$ for $n = 1$, Eq. (3), due to the deviations from the exact sudden limit.

For completeness, we also consider the leading-order correction to the sudden limit. To do so, a first-order time-dependent perturbation theory is employed with respect to H_k around the exact sudden-quench solution. This shows that the leading-order correction to all cumulants scales as $\delta\kappa_q^{(n)}(T) \propto T n^{-3}$. As a result, the CD fast-quench regime is established when the correction becomes comparable to the universal value of the cumulants in the sudden limit $\delta\kappa_q^{(n)}(T) \sim n^{-1} \rightarrow T_{\text{CD}}^{\text{fast}} \sim n^2$. In particular, as shown in [55], the first three cumulants are given by $\delta\kappa_1^{(n)}(T) \approx -0.7 T n^{-3}$, $\delta\kappa_2^{(n)}(T) \approx -1.5 T n^{-3}$, $\delta\kappa_3^{(n)}(T) \approx -3.55 T n^{-3}$. As shown in Fig. 3, the first-order correction accurately captures almost the complete crossover between the slow and fast driving limits. The main result for the fast quench cumulant scaling, Eq. (6), also reveals further exact features regarding adiabatic dynamics. The onset of adiabaticity can be captured by $\kappa_1^{(n)}(0) = 2/L$ defining the adiabatic threshold value of the CD expansion order, $n_{\text{ad}}^{\text{CD}} \approx \frac{1.05}{2\pi} L$. Thus, adiabaticity emerges when the dynamics is assisted by a local CD expansion of significantly lower order than that of the exact CD protocol, $n = L$. This justifies the efficiency of approximate local CD protocols. Above this threshold, defect formation is restricted to the zero mode in the leading order, and the ground-state fidelity, otherwise exponentially small with L , becomes finite. As a result, the CD fast-quench plateau is then equivalent to a quasi-adiabatic regime, while the CD fast-quench breakdown results in reaching the adiabatic limit $T_{\text{ad}}^{\text{CD}} \approx T_{\text{fast}}^{\text{CD}}$.

The exact results in the fast quench regime also allow for approximate analytical characterization for driving times beyond the CD fast quench breakdown, $T > T_{\text{fast}}^{\text{CD}}$ and above the CD onset of adiabaticity, $n < n_{\text{ad}}$. As detailed in [55], the cumulant generating function can be accurately captured by truncating the sum of the independent Landau-Zener excitations up to momentum $k_n \propto 1/n$, $\log \hat{P}^{(n)}(\theta; T) \approx -L (8\pi^2 T)^{-1/2} \sum_{p=1}^{\infty} \frac{(1-e^{i\theta})^p}{p^{3/2}} \text{erf}(\sqrt{2\pi p} k_n)$. Beyond the CD fast quench breakdown scale, the dynamics is insensitive to CD, and the KZ cumulant scaling remains unchanged. Moreover, requiring that the corresponding average defect number $\kappa_1^{(n)}(T) \approx$

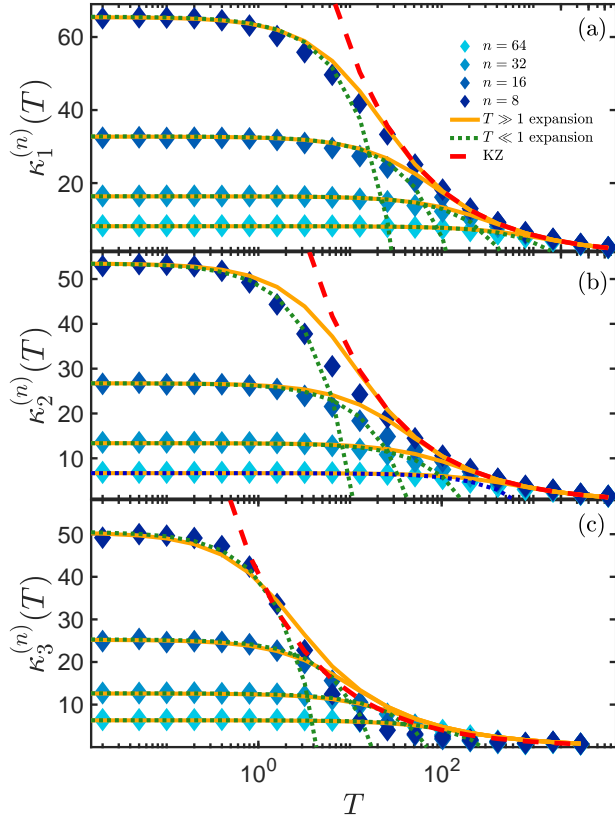


FIG. 3. (a) Average, (b) variance, and (c) skewness of the defect statistics for CD expansion orders $n = 8, 16, 32, 64$ and $L = 1600$. The first-order correction around the sudden limit provides a slightly more accurate description of the CD intermediate regime than the analytical ansatz from the slow driving limit.

$L(8\pi^2 T)^{-1/2} \text{erf}(\sqrt{2\pi p} k_n)$ converges to the fast-quench plateau for $T \rightarrow 0$ can be used to fix the cut-off momentum as $k_n \approx 1.05/n$. This provides a highly accurate interpolation between the slow and fast regimes and captures the non-universal properties around the CD fast-quench breakdown. Remarkably, this construction can be further generalized as an ansatz by requiring that all cumulants converge to the limiting values in the fast quench regime,

$$\kappa_q^{(n)}(T) \approx L \kappa_q^{\text{KZ}}(T) \text{erf} \left[\frac{\sqrt{\pi} \kappa_q^{(n)}(0)}{2\kappa_q^{\text{KZ}}(T)} \right], \quad (7)$$

with $\kappa_q^{\text{KZ}}(T)$ denoting the KZ scaling of the q -th cumulant. As shown in Fig. 3, Eq. (7) provides an excellent fit to the numerical results in the crossover regime between the fast and slow limits.

Universality. The analytical arguments behind the fast quench breakdown and cumulant scaling can be extended to arbitrary critical systems with a second-order QPT in d dimensions and of linear size L . As a feasible ap-

proximation, we assume that excess energy is gradually generated by $D < d$ dimensional defects with finite spatial separation appearing at the interfaces of frozen domains. Consequently, the n -th order local CD expansion can be interpreted as approximately enforcing adiabatic evolution within domains of size $\sim n^d$. Thus, their number scales as L^d/n^d , leaving room for defect generation at $L^d/n^d \times n^D \sim L^d n^{-(d-D)}$ positions. Assuming that this happens independently [12] according to a Poisson-binomial distribution, all defect cumulants will be proportional to the number of locations where defects can be formed,

$$\kappa_q^{(n)}(0) \propto n^{-(d-D)}. \quad (8)$$

To demonstrate this universal scaling law on a more quantitative level, consider the broad class of quantum critical Hamiltonians $H(t) = \sum_{\mathbf{k}} \hat{\varphi}_{\mathbf{k}} H_{\mathbf{k}}(t) \hat{\varphi}_{\mathbf{k}}^\dagger$, $\hat{\varphi}_{\mathbf{k}} = (c_{-\mathbf{k}}, c_{\mathbf{k}}^\dagger)$ in d spatial dimensions with $\epsilon_{\mathbf{k}} \sim |\mathbf{k}|^z$ in which Landau-Zener transitions properly describe defect formation in slow quenches, equivalent to $z\nu = 1$. The exact CD term of the \mathbf{k} -th mode can generally be expressed as $q_{\mathbf{k}}(t) = f(\mathbf{k})/(T\epsilon_{\mathbf{k}}^2)$ with the bounded function $f(\mathbf{k})$ encoding the \mathbf{k} -th mode of the interactions. The n -th order of the Krylov expansion $q_{\mathbf{k}}^{(n)}(t)$ comes from the linear combination of the nested commutators up to the order $2n - 1$, which scales up the interaction range by a factor $\sim n$, regardless of the dimensionality. Thus, the following scaling is expected, $q_{\mathbf{k}}^{(n)}(t) \sim \sum_{m=1}^n f_m(m\mathbf{k})/(T\epsilon_{\mathbf{k}}^2)$ as the stretched interactions amplify the corresponding mode expansion, while the denominator accounts for the overall magnitude near the critical point. Consequently, the analytical argument in the TFIM [55] can be generalized to D dimensional defects [56–58]. For $|\mathbf{k}| \gtrsim 1/n$ the numerator remains finite implying that for $T \gg n^{2z}$ both the CD term is eliminated, $q_{\mathbf{k}}^{(n)}(t) \sim 1/(T|\mathbf{k}|^{2z}) \ll 1$ and the Landau-Zener transitions are suppressed as $-\log p_{\mathbf{k}} \sim T|\mathbf{k}|^{2z} \gg 1$. In the opposite limit, $T \ll n^{2z}$, the CD term dominates and $q_{\mathbf{k}}^{(n)}(t) \sim 1/(T|\mathbf{k}|^{2z}) \gg 1$, implying adiabatic dynamics again. As a result, the n -th order CD expansion universally restricts the dynamics below the cut-off momentum $|\mathbf{k}_n| \lesssim 1/n$. This implies the universal CD fast quench scale $T_{\text{fast}}^{\text{CD}} \sim n^{2z}$, below which defect formation is unaltered, $\kappa_q^{(n)}(T) \sim T^{-\frac{d-D}{2z}}$. The fast quench plateau is obtained by summing up the saturated transition probabilities $p_{\mathbf{k}} \sim O(1)$ for all possible momenta up to $|\mathbf{k}_n| \sim 1/n$ across the D -dimensional critical surface. This yields a universal scaling for all cumulants of the form $\kappa_q^{(n)}(0) \sim \int_0^{|\mathbf{k}_n|} d^{d-D} \mathbf{k} p_{\mathbf{k}} \propto n^{-(d-D)}$. This framework applies to critical systems regardless of whether the KZ mechanism or a more general dynamical power-law scaling describes the average defect generation. The former is perfectly mirrored by the TFIM, while the more general case of the latter can be demonstrated via approximate methods in the long-range Kitaev models [55].

Conclusions.— Counterdiabatic driving provides a powerful approach to suppress excitations in driven systems, but its performance has remained elusive under approximate protocols with a tailored locality required to ease their implementation. Our findings establish exact analytical results for the defect statistics regardless of the driving rate and for an arbitrary CD expansion order. In the fast quench regime, all cumulants are proportional, universally scaling with the inverse of the CD expansion order, depending solely on the dimensionality of the systems and the defects. In addition, universal signatures of the defect statistics are also present away from the sudden limit, for arbitrary driving times. Our analytical findings thus provide a theoretical framework for understanding the efficiency of local CD protocols with broad implications for quantum simulation, control of quantum matter, quantum thermodynamics, and counterdiabatic quantum algorithms.

Acknowledgments. This project was supported by the Luxembourg National Research Fund (FNR Grant Nos. 17132054 and 16434093). It has also received funding from the QuantERA II Joint Programme and co-funding from the European Union’s Horizon 2020 research and innovation programme.

* andras.grabarits@uni.lu

- [1] S. Sachdev, *Quantum Phase Transitions*, 2nd ed. (Cambridge University Press, 2011).
- [2] T. Kato, On the Adiabatic Theorem of Quantum Mechanics, *J. Phys. Soc. Japan* **5**, 435 (1950).
- [3] S. Jansen, M.-B. Ruskai, and R. Seiler, Bounds for the adiabatic approximation with applications to quantum computation, *J. Math. Phys.* **48**, 102111 (2007).
- [4] J. I. Cirac and P. Zoller, Goals and opportunities in quantum simulation, *Nature Physics* **8**, 264 (2012).
- [5] T. Albash and D. A. Lidar, Adiabatic quantum computation, *Rev. Mod. Phys.* **90**, 015002 (2018).
- [6] P. Doria, T. Calarco, and S. Montangero, Optimal control technique for many-body quantum dynamics, *Phys. Rev. Lett.* **106**, 190501 (2011).
- [7] N. Wu, A. Nanduri, and H. Rabitz, Optimal suppression of defect generation during a passage across a quantum critical point, *Phys. Rev. B* **91**, 041115 (2015).
- [8] D. Sen, K. Sengupta, and S. Mondal, Defect Production in Nonlinear Quench across a Quantum Critical Point, *Phys. Rev. Lett.* **101**, 016806 (2008).
- [9] R. Barankov and A. Polkovnikov, Optimal Nonlinear Passage Through a Quantum Critical Point, *Phys. Rev. Lett.* **101**, 076801 (2008).
- [10] J. Dziarmaga, Dynamics of a quantum phase transition and relaxation to a steady state, *Advances in Physics* **59**, 1063 (2010).
- [11] M. Collura and D. Karevski, Critical quench dynamics in confined systems, *Phys. Rev. Lett.* **104**, 200601 (2010).
- [12] F. J. Gómez-Ruiz, J. J. Mayo, and A. del Campo, Full counting statistics of topological defects after crossing a phase transition, *Phys. Rev. Lett.* **124**, 240602 (2020).
- [13] J. D. Sau and K. Sengupta, Suppressing defect production during passage through a quantum critical point, *Phys. Rev. B* **90**, 104306 (2014).
- [14] M. M. Rams, J. Dziarmaga, and W. H. Zurek, Symmetry breaking bias and the dynamics of a quantum phase transition, *Phys. Rev. Lett.* **123**, 130603 (2019).
- [15] K. Hódsági and M. Kormos, Kibble–Zurek mechanism in the Ising Field Theory, *SciPost Phys.* **9**, 055 (2020).
- [16] B. Dóra, M. Heyl, and R. Moessner, The kibble-zurek mechanism at exceptional points, *Nature Communications* **10**, 2254 (2019).
- [17] E. C. King, J. N. Kriel, and M. Kastner, Universal cooling dynamics toward a quantum critical point, *Phys. Rev. Lett.* **130**, 050401 (2023).
- [18] Á. Bácsi and B. Dóra, Kibble–zurek scaling due to environment temperature quench in the transverse field ising model, *Scientific Reports* **13**, 4034 (2023).
- [19] S. Mahunta and V. Mukherjee, Shortcuts to adiabaticity in open quantum critical systems, *Phys. Rev. B* **111**, 064301 (2025).
- [20] U. Divakaran, A. Dutta, and D. Sen, Quenching along a gapless line: A different exponent for defect density, *Phys. Rev. B* **78**, 144301 (2008).
- [21] S. Deng, G. Ortiz, and L. Viola, Anomalous nonergodic scaling in adiabatic multicritical quantum quenches, *Phys. Rev. B* **80**, 241109 (2009).
- [22] B. Yan, V. Y. Chernyak, W. H. Zurek, and N. A. Sinitsyn, Nonadiabatic phase transition with broken chiral symmetry, *Phys. Rev. Lett.* **126**, 070602 (2021).
- [23] M. Demirplak and S. A. Rice, Adiabatic Population Transfer with Control Fields, *J. Phys. Chem. A* **107**, 9937 (2003).
- [24] M. Demirplak and S. A. Rice, Assisted Adiabatic Passage Revisited, *J. Phys. Chem. B* **109**, 6838 (2005).
- [25] M. Demirplak and S. A. Rice, On the consistency, extremal, and global properties of counterdiabatic fields, *J. Chem. Phys.* **129**, 154111 (2008).
- [26] M. V. Berry, Transitionless quantum driving, *J. Phys. A* **42**, 365303 (2009).
- [27] A. del Campo, M. M. Rams, and W. H. Zurek, Assisted Finite-Rate Adiabatic Passage Across a Quantum Critical Point: Exact Solution for the Quantum Ising Model, *Phys. Rev. Lett.* **109**, 115703 (2012).
- [28] K. Takahashi, Transitionless quantum driving for spin systems, *Phys. Rev. E* **87**, 062117 (2013).
- [29] B. Damski, Counterdiabatic driving of the quantum Ising model, *J. Stat. Mech. Theory Exp.* **2014**, P12019 (2014).
- [30] H. Saberi, T. Opatrný, K. Mølmer, and A. del Campo, Adiabatic tracking of quantum many-body dynamics, *Phys. Rev. A* **90**, 060301 (2014).
- [31] D. Sels and A. Polkovnikov, Minimizing irreversible losses in quantum systems by local counterdiabatic driving, *Proceedings of the National Academy of Sciences* **114**, E3909 (2017).
- [32] P. W. Claeys, M. Pandey, D. Sels, and A. Polkovnikov, Floquet-Engineering Counterdiabatic Protocols in Quantum Many-Body Systems, *Phys. Rev. Lett.* **123**, 090602 (2019).
- [33] K. Takahashi and A. del Campo, Shortcuts to Adiabaticity in Krylov Space, *Phys. Rev. X* **14**, 011032 (2024).
- [34] B. Bhattacharjee, A Lanczos approach to the Adiabatic Gauge Potential (2023), [arXiv:2302.07228](https://arxiv.org/abs/2302.07228).
- [35] A.-M. Visuri, A. G. Cadavid, B. A. Bhargava, S. V.

- Romero, A. Grabarits, P. Chandarana, E. Solano, A. del Campo, and N. N. Hegade, [Digitized counterdiabatic quantum critical dynamics](#) (2025), [arXiv:2502.15100 \[quant-ph\]](#).
- [36] W. H. Zurek, U. Dorner, and P. Zoller, Dynamics of a Quantum Phase Transition, *Phys. Rev. Lett.* **95**, 105701 (2005).
- [37] J. Dziarmaga, Dynamics of a Quantum Phase Transition: Exact Solution of the Quantum Ising Model, *Phys. Rev. Lett.* **95**, 245701 (2005).
- [38] S. Suzuki, J. Inoue, and B. Chakrabarti, *Quantum Ising Phases and Transitions in Transverse Ising Models*, Lecture Notes in Physics (Springer, 2012).
- [39] B. Damski, The Simplest Quantum Model Supporting the Kibble-Zurek Mechanism of Topological Defect Production: Landau-Zener Transitions from a New Perspective, *Phys. Rev. Lett.* **95**, 035701 (2005).
- [40] B. Damski and W. H. Zurek, Adiabatic-impulse approximation for avoided level crossings: From phase-transition dynamics to Landau-Zener evolutions and back again, *Phys. Rev. A* **73**, 063405 (2006).
- [41] T. W. B. Kibble, Topology of cosmic domains and strings, *Journal of Physics A Mathematical General* **9**, 1387 (1976).
- [42] T. Kibble, Some implications of a cosmological phase transition, *Physics Reports* **67**, 183 (1980).
- [43] W. H. Zurek, Cosmological experiments in superfluid helium?, *Nature* **317**, 505 (1985).
- [44] W. Zurek, Cosmological experiments in condensed matter systems, *Physics Reports* **276**, 177 (1996).
- [45] A. del Campo and W. H. Zurek, Universality of phase transition dynamics: Topological defects from symmetry breaking, *International Journal of Modern Physics A* **29**, 1430018 (2014).
- [46] H.-B. Zeng, C.-Y. Xia, and A. del Campo, Universal Breakdown of Kibble-Zurek Scaling in Fast Quenches across a Phase Transition, *Phys. Rev. Lett.* **130**, 060402 (2023).
- [47] A. Grabarits, F. Balducci, and A. del Campo, [Driving a quantum phase transition at arbitrary rate: Exact solution of the transverse-field ising model](#) (2025), [arXiv:2501.10478 \[cond-mat.stat-mech\]](#).
- [48] L. Cincio, J. Dziarmaga, M. M. Rams, and W. H. Zurek, Entropy of entanglement and correlations induced by a quench: Dynamics of a quantum phase transition in the quantum ising model, *Phys. Rev. A* **75**, 052321 (2007).
- [49] A. del Campo, Universal statistics of topological defects formed in a quantum phase transition, *Phys. Rev. Lett.* **121**, 200601 (2018).
- [50] J.-M. Cui, F. J. Gómez-Ruiz, Y.-F. Huang, C.-F. Li, G.-C. Guo, and A. del Campo, Experimentally testing quantum critical dynamics beyond the kibble-zurek mechanism, *Communications Physics* **3**, 44 (2020).
- [51] F. Balducci, M. Beau, J. Yang, *et al.*, Large Deviations beyond the Kibble-Zurek Mechanism, *Phys. Rev. Lett.* **131**, 230401 (2023).
- [52] Y. Bando, Y. Susa, H. Oshiyama, *et al.*, Probing the universality of topological defect formation in a quantum annealer: Kibble-Zurek mechanism and beyond, *Phys. Rev. Research* **2**, 033369 (2020).
- [53] Y. Bando and H. Nishimori, Simulated quantum annealing as a simulator of nonequilibrium quantum dynamics, *Phys. Rev. A* **104**, 022607 (2021).
- [54] A. D. King, S. Suzuki, J. Raymond, *et al.*, Coherent quantum annealing in a programmable 2,000-qubit Ising chain, *Nat. Phys.* **18**, 1324 (2022).
- [55] See Supplemental Material at URL-will-be-inserted-by-publisher for the data of the experiments.
- [56] S. Mondal, D. Sen, and K. Sengupta, Quench dynamics and defect production in the kitaev and extended kitaev models, *Phys. Rev. B* **78**, 045101 (2008).
- [57] S. Sarkar, D. Rana, and S. Mandal, Defect production and quench dynamics in the three-dimensional kitaev model, *Phys. Rev. B* **102**, 134309 (2020).
- [58] F. Zhang and H. T. Quan, Work statistics across a quantum critical surface, *Phys. Rev. E* **105**, 024101 (2022).
- [59] N. Defenu, G. Morigi, L. Dell’Anna, and T. Enss, Universal dynamical scaling of long-range topological superconductors, *Phys. Rev. B* **100**, 184306 (2019).

EXACT TIME-EVOLUTION WITH CD IN THE FAST QUENCH REGIME

In this section, we provide the details of the analytical calculations of the exact time-evolved states of the TLSs for fast quenches in the presence of arbitrary order of CD. In this limit, the time evolution is generated only by the CD term,

$$\partial_t \begin{bmatrix} \psi_{k,1}(t) \\ \psi_{k,2}(t) \end{bmatrix} = -i q_k^{(n)}(t) \tau^y \begin{bmatrix} \psi_{k,1}(t) \\ \psi_{k,2}(t) \end{bmatrix} \Rightarrow \begin{bmatrix} \psi_{k,1}(T) \\ \psi_{k,2}(T) \end{bmatrix} = e^{-i \int_0^T dt' q_k^{(n)}(t') \tau^y} \begin{pmatrix} 0 \\ 1 \end{pmatrix}, \quad (9)$$

where $q_k^{(n)}(t) = -\dot{g} \sum_{m=1}^n \frac{\sin(km)}{2} \frac{g^{2m}(1+g^L)}{g^{m+1}+g^L}$ from the results of Ref. [39]. For brevity, we omitted the n -dependence of the wave-function components. In the second step, the time-evolution operator could be expressed as the exponential of the CD Hamiltonian as the time-dependence appears only by a multiplying factor. Exploiting the property of $(\tau^y)^{2n} = \mathbb{I}_2$ and $(\tau^y)^{2n+1} = \tau^y$

$$e^{-i \int_0^T dt' q_k^{(n)}(t') \tau^y} \begin{pmatrix} 0 \\ 1 \end{pmatrix} = \left[\cos \left[\int_0^T dt' q_k^{(n)}(t') \right] - i \sin \left[\int_0^T dt' q_k^{(n)}(t') \right] \tau^y \right] \begin{pmatrix} 0 \\ 1 \end{pmatrix} = \begin{bmatrix} -\sin \left[\int_0^T dt' q_k^{(n)}(t') \right] \\ \cos \left[\int_0^T dt' q_k^{(n)}(t') \right] \end{bmatrix}. \quad (10)$$

Note that this limit simplifies the calculation to a huge extent given that $q_k^n(t)$ is proportional to the derivative \dot{g} . So the phases are simply the integrals according to the control parameter itself, by the simple identity $-\int_0^T dt \dot{g} \dots = \int_0^{g_0} dg \dots$. In particular, for the Krylov expansion and with the exact formula for the off-diagonal matrix elements, we have

$$\begin{aligned} \varphi_k^{(n)}(T) &\equiv \int_0^T dt' q_k^{(n)}(t') = \frac{1}{2} \sum_m \sin(km) \int_0^{g_0} dg \frac{g^{m-1} + g^{L-m-1}}{1+g^L} \approx \frac{1}{2} \sum_m \sin(km) \left(\int_0^1 dg g^{m-1} + \int_1^{g_0} dg g^{-m-1} \right) \\ &= \frac{1}{2} \sum_{m=1}^n \frac{\sin(km)}{m} (2 - g_0^{-m}) \approx - \sum_{m=0}^{\infty} \frac{\sin[k(n+m+1)]}{n+m} + \frac{\pi - k}{2}, \end{aligned} \quad (11)$$

where in the last step the power of the initial transverse field was neglected, $g_0^{-m} \approx 0$. Additionally, we also employed the approximation of $g^L \approx 0$, $\frac{g^{m-1} + g^{L-m-1}}{1+g^L} \approx g^{m-1}$ for $|g| < 1$, and $\frac{g^L}{1+g^L} \approx 1$, $\frac{g^{m-1} + g^{L-m-1}}{1+g^L} \approx g^{-m-1}$ for $|g| > 1$. Although it is a complicated expression, it is instructive to write out for the first two orders,

$$\begin{bmatrix} \psi_{k,1}(T) \\ \psi_{k,2}(T) \end{bmatrix} = \begin{bmatrix} -\sin \left[\varphi_k^{(1)}(T) \right] \\ \cos \left[\varphi_k^{(1)}(T) \right] \end{bmatrix} = \begin{bmatrix} -\sin(\sin k) \\ \cos(\sin k) \end{bmatrix}, \quad (12)$$

$$\begin{bmatrix} \psi_{k,1}(T) \\ \psi_{k,2}(T) \end{bmatrix} = \begin{bmatrix} -\sin \left[\varphi_k^{(2)}(T) \right] \\ \cos \left[\varphi_k^{(2)}(T) \right] \end{bmatrix} = \begin{bmatrix} -\sin \left[\sin k + \frac{\sin(2k)}{2} \right] \\ \cos \left[\sin k + \frac{\sin(2k)}{2} \right] \end{bmatrix}. \quad (13)$$

The corresponding excitation probabilities are given by

$$p_k^{(1)} \approx \left| \sin \frac{k}{2} \psi_{k,1}(T) + \cos \frac{k}{2} \psi_{k,2}(T) \right|^2 \approx \sin^2 \frac{k}{2} \sin^2(\sin k) + \cos^2 \frac{k}{2} \cos^2(\sin k) - \frac{1}{2} \sin k \sin(2 \sin k), \quad (14)$$

$$p_k^{(2)} \approx \sin^2 \frac{k}{2} \sin^2 \left[\sin k + \frac{\sin(2k)}{2} \right] + \cos^2 \frac{k}{2} \cos^2 \left[\sin k + \frac{\sin(2k)}{2} \right] - \frac{1}{2} \sin k \sin[2 \sin k + \sin(2k)]. \quad (15)$$

In the large CD order limit, we exploit the last expression of Eq. (11) to reveal the universal properties of the defect cumulants. The fast quench universal regime is captured by the leading order expansion in terms of the expansion order of CD, n . Next, we expand the $\sin[\varphi_k^{(n)}(T)]$ and $\cos[\varphi_k^{(n)}(T)]$ around $(\pi - k)/2$ as only the part $-\sum_{m=0}^{\infty} \frac{\sin[k(n+m+1)]}{n+m}$ in the phase $\varphi_k^n(T)$ is responsible for non-adiabatic effects,

$$\begin{bmatrix} \psi_{k,1}(T) \\ \psi_{k,2}(T) \end{bmatrix} = \begin{bmatrix} -\sin \left[\varphi_k^{(n)}(T) \right] \\ \cos \left[\varphi_k^{(n)}(T) \right] \end{bmatrix} \quad (16)$$

$$= \begin{bmatrix} -\cos \frac{k}{2} \cos \left[\sum_{m=0}^{\infty} \frac{\sin[k(n+m+1)]}{n+m} \right] + \sin \frac{k}{2} \sin \left[\sum_{m=0}^{\infty} \frac{\sin[k(n+m+1)]}{n+m} \right] \\ \sin \frac{k}{2} \cos \left[\sum_{m=0}^{\infty} \frac{\sin[k(n+m+1)]}{n+m} \right] - \cos \frac{k}{2} \sin \left[\sum_{m=0}^{\infty} \frac{\sin[k(n+m+1)]}{n+m} \right] \end{bmatrix}. \quad (17)$$

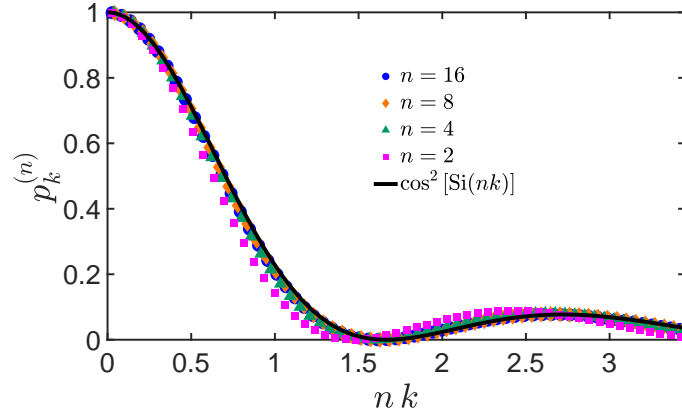


FIG. 4. Fast quench excitation probabilities for various orders of CD expansion, $n = 2, 4, 8, 16$ and $T = 2$ showing a precise scaling collapse as a function of $n k$ even for $n = 2$, $L = 1600$ and matching well with the limiting function $p_k^{(n)} \approx \cos^2 [\text{Si}(nk)]$.

In the excitation probabilities, the first terms in the wave function cancel exactly, leaving us with a compact expression of

$$p_k^{(n)} \approx \left| \sin \frac{k}{2} \psi_{k,1}(T) + \cos \frac{k}{2} \psi_{k,2}(T) \right|^2 = \sin^2 \left[\sum_{m=0}^{\infty} \frac{\sin[k(n+m+1)]}{n+m} \right] \cos^2 k. \quad (18)$$

Next, we show the derivation of the universal scaling of the excitation probabilities, Eq. (18). For this, we employ an integral approximation of the term $-\sum_{m=0}^{\infty} \frac{\sin[k(n+m+1)]}{n+m}$. Introducing the rescaled momentum, $\kappa = nk$,

$$\begin{aligned} \sum_{m=n}^{\infty} \frac{\sin\left(\kappa \frac{m}{n}\right)}{m-1} &\approx \int_{1+\frac{1}{n}}^{\infty} dx \frac{\sin(\kappa x)}{x - \frac{1}{n}} = \int_1^{\infty} dx \frac{\sin(\kappa x)}{x} + \frac{1}{n} \int_1^{\infty} dx \frac{\sin(\kappa x)}{x^2} - \frac{1}{n} \sin(\kappa) + O(1/n^2) \\ &\approx \frac{1}{2} \pi - \text{Si}(\kappa) + \frac{\kappa}{n} \text{Ci}(\kappa). \end{aligned} \quad (19)$$

Here the sine and cosine integral functions have been introduced as $\text{Si}(z) = \int_0^z dt \frac{\sin t}{t}$ and $\text{Ci}(z) = -\int_z^{\infty} dt \frac{\cos t}{t}$, respectively. Next, we expand the outer sine function as

$$\begin{aligned} \sin^2 \left[\frac{\pi}{2} - \text{Si}(\kappa) + \frac{\kappa}{n} \text{Ci}(\kappa) \right] &= \left[\sin \frac{\pi}{2} \cos [\text{Si}(\kappa)] - \cos \frac{\pi}{2} \sin [\text{Si}(\kappa)] \right]^2 \\ &= \cos^2 \left[\text{Si}(\kappa) + \frac{\kappa}{n} \text{Ci}(\kappa) \right] \approx \cos^2 (\text{Si}(\kappa)) - \frac{\kappa}{n} \text{Ci}(\kappa) \sin [2\text{Si}(\kappa)]. \end{aligned} \quad (20)$$

The final excitation probabilities come from Eq. (18)

$$p_k^{(n)} \approx \left| \sin \frac{k}{2} \psi_{k,1}(T) + \cos \frac{k}{2} \psi_{k,2}(T) \right|^2 = \cos^2 [\text{Si}(\kappa)] \cos^2 k \approx \cos^2 [\text{Si}(\kappa)], \quad (21)$$

where in the last step we have taken $\cos^2 k = \cos^2(\kappa/n) \approx 1$, as for large enough $n \gtrsim \sqrt{L}/10$, the cosine argument goes to zero. The precise matching with the analytical results, Eq. (21) and the scaling collapse for different values of n are shown in Fig. 4. The overall matching with the analytical formula for small and moderate driving times are further demonstrated in Fig. 5

Finally, we demonstrate the precision of this approximation by the wave-function components as a function k for CD order $n = 64$. The time-involved wave-function with the original expression of $\varphi_k^{(n)}(T)$ reads as

$$\begin{bmatrix} \psi_{k,1}(T) \\ \psi_{k,2}(T) \end{bmatrix} = \begin{bmatrix} -\sin [\text{Si}(nk) - k/2] \\ \cos [\text{Si}(nk) - k/2] \end{bmatrix}. \quad (22)$$

The matching with the numerical results are shown in Fig. 6, precisely reproducing the highly non-trivial oscillatory behavior.

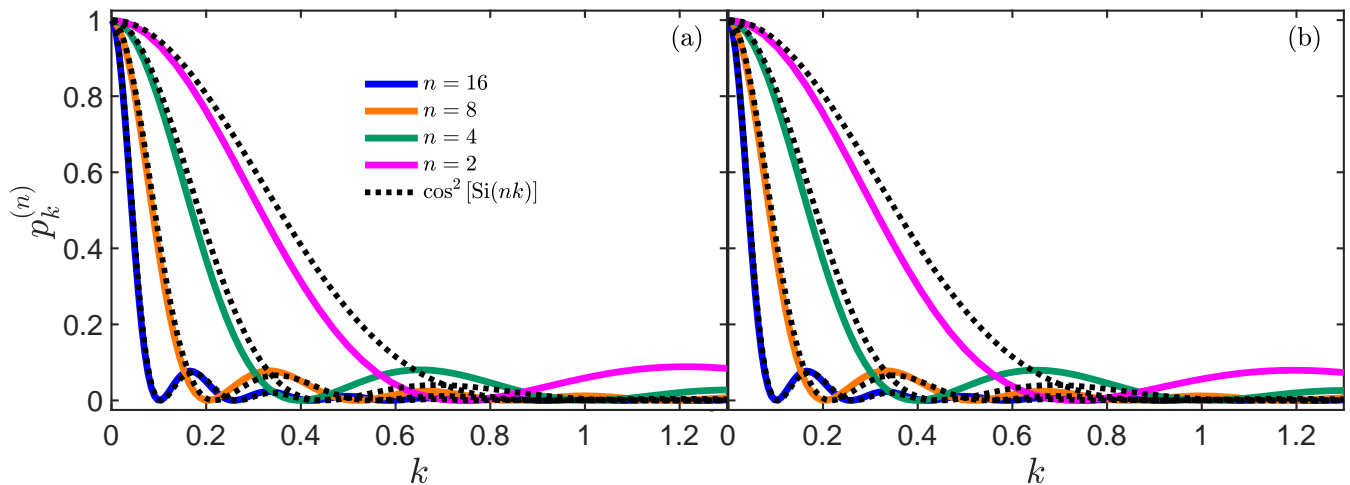


FIG. 5. Fast quench excitation probabilities for various orders of CD expansion, $n = 2, 4, 8, 16$ showing good matching with the limiting function, in Eq. (21) for both $T = 10^{-6}$ in the sudden quench limit, (a) and even close to the crossover regime, $T = 4$, (b). The approximating form of $p_k^{(n)}$ captures well the dominating part even for the lowest order expansion, $n = 2, L = 1600$.

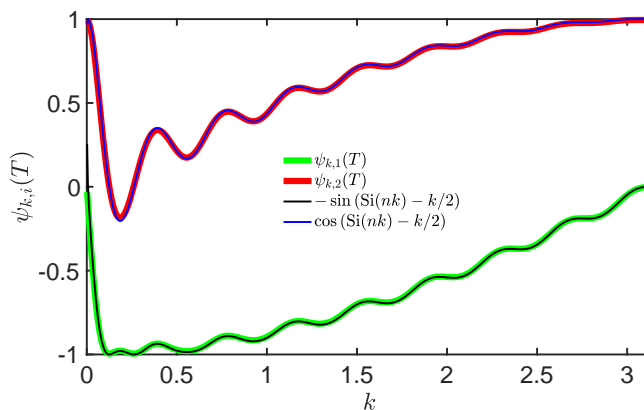


FIG. 6. Time-evolved wave-function components at the end of the time-evolution precisely matching the analytical results for $L = 1600, n = 64, T = 10^{-3}$.

CUMULANT RATIOS

In this section, we further demonstrate how the defect cumulant ratios in the TFIM change between the fast and slow driving regimes for various CD expansion orders. As demonstrated in Fig. 7a, the ratios of κ_2/κ_1 interpolate smoothly between the constant plateaus of the fast quench and the slow driving limit. In the former case, the limiting ratio for large enough n is approximately $\kappa_2/\kappa_1 \approx 0.82$ while without CD it is given by $\kappa_2/\kappa_1 \approx 0.5$. In the latter, the ratio converges to the KZ scaling limit for driving time exceeding the CD fast quench breakdown, $T \gg n^2$. However, the KZ scaling limit only emerges provided that CD non-locality is below the CD adiabatic limit $n < n_{\text{ad}}^{\text{CD}}$. Similar findings are presented in Fig. 7b for the skewness ratios under the same conditions. The limiting ratio values are given by $\kappa_3/\kappa_1 \approx 0.132$ in the KZ scaling limit and $\kappa_3/\kappa_1 \approx 0.76$ in the fast quench limit for large enough n while it converges to zero without CD. In both figures we also demonstrate that the leading order expansion around the sudden limit accurately captures the dominating part of the crossover regime.

LEADING ORDER EXPANSION AROUND THE SUDDEN LIMIT

In this section, we provide the leading order correction with respect to the bare Hamiltonian around the sudden limit, Eq. (22). To do so, we transform the time-dependent Schrödinger equation into Dirac picture with respect to

the time-evolution generated by the CD term,

$$\begin{bmatrix} \psi_{n,1}(t) \\ \psi_{n,2}(t) \end{bmatrix} = U_n \begin{bmatrix} \psi_{k,1}(t) \\ \psi_{k,2}(t) \end{bmatrix}, \quad (23)$$

where for brevity we have again omitted the n dependencies and denoted the wave-function components in the Dirac picture by $\psi_{n,1}$ and $\psi_{n,2}$, respectively. Here U_n is the inverse of the CD time-evolution operator, given in Eq. (10), given by

$$U_n = \cos [\varphi^{(n)}(t)] + i \sin [\varphi^{(n)}(t)] \tau^y, \quad (24)$$

where $\varphi^{(n)}(t) = \int_0^t dt' q^{(n)}(t')$, which is given by changing to the variable g

$$\varphi^{(n)}(g) \approx \sum_{m=1}^n \frac{\sin(km)}{m} g^m. \quad (25)$$

The corresponding time-dependent Schrödinger equation in the Dirac picture is given by

$$\partial_t \begin{bmatrix} \psi_{n,1}(t) \\ \psi_{n,2}(t) \end{bmatrix} = -i U_n H(t) U_n^\dagger \begin{bmatrix} \psi_{n,1}(t) \\ \psi_{n,2}(t) \end{bmatrix}. \quad (26)$$

Next, we evaluate the generator by exploiting that $\tau^y \tau^{x,z} \tau^y = -\tau^{x,z}$ and $\tau^y \tau^{x,z} = -\tau^{x,z} \tau^y$, leading to

$$\begin{aligned} U_n H(t) U_n^\dagger &= H(t) \left\{ \cos^2 [\varphi^{(n)}(t)] - \sin^2 [\varphi^{(n)}(t)] - 2i \cos [\varphi^{(n)}(t)] \sin [\varphi^{(n)}(t)] \tau^y \right\} \\ &= H(t) \left\{ \cos [2\varphi^{(n)}(t)] - i \sin [2\varphi^{(n)}(t)] \tau^y \right\} = H(t) e^{-2i \varphi^{(n)}(t) \tau^y}. \end{aligned} \quad (27)$$

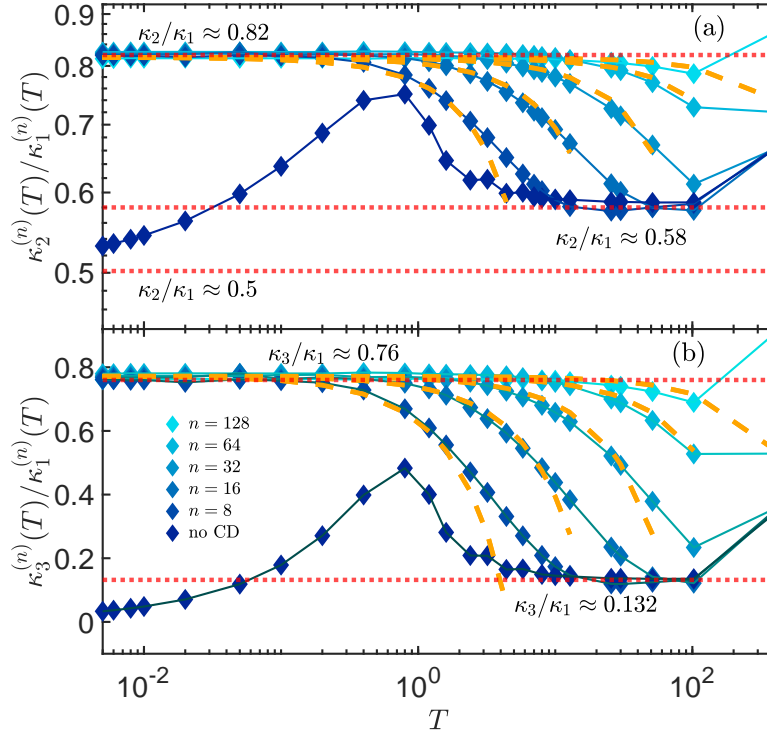


FIG. 7. Cumulant ratios as a function of the driving time for various orders of CD expansion, $n = 0, 8, 16, 32, 64, 128$. (a): the variance ratio κ_2/κ_1 exhibits a smooth crossover between the fast quench plateaus with and without CD and the CD independent KZ scaling limit. (b): Similar findings for the skewness ratio, κ_3/κ_1 with no CD converging to zero in the fast quench regime. Orange dashed lines denote the leading order expansion around the sudden limit.

Thus, the leading order correction within the time-dependent perturbation theory in terms of the time-evolution operator at the end of the process, $t = T$ is given

$$U^D(T) \approx \mathbb{I}_2 + iT \int_0^{g_0} dg [(g - \cos k)\tau^z + \sin k\tau^x] \exp \left[-2i \sum_{m=1}^n \frac{\sin(km)}{m} g^m \tau^y \right]. \quad (28)$$

By employing the same integral approximation as in Eq. (19), the wave-function components in the Dirac picture can be written as

$$\begin{aligned} \begin{bmatrix} \psi_{1,n}(T) \\ \psi_{2,n}(T) \end{bmatrix} = & \quad (29) \\ \left\{ \cos \left[\sum_{m=1}^n \frac{\sin(km)}{m} \right] - i \sin \left[\sum_{m=1}^n \frac{\sin(km)}{m} \right] \tau^y \right\} & \left\{ \mathbb{I}_2 + iT \int_0^{g_0} dg H(g) \exp \left[-2i \sum_{m=1}^n \frac{\sin(km)}{m} g^m \tau^y \right] \right\} \begin{pmatrix} 0 \\ 1 \end{pmatrix} \\ \approx \begin{bmatrix} -\sin [\text{Si}(nk) - k/2] \\ \cos [\text{Si}(nk) - k/2] \end{bmatrix} + iT \int_0^{g_0} dg & H(g) \exp \left[-i \sum_{m=1}^n \frac{\sin(km)}{m} (2g^m - 1) \tau^y \right] \begin{pmatrix} 0 \\ 1 \end{pmatrix} \\ \approx \begin{bmatrix} -\sin [\text{Si}(nk) - k/2] \\ \cos [\text{Si}(nk) - k/2] \end{bmatrix} + iT \int_0^{g_0} dg & \begin{bmatrix} (\cos k - g) \sin \left[\sum_{m=1}^n \frac{\sin(km)}{m} (2g^m - 1) \right] + \sin k \cos \left[\sum_{m=1}^n \frac{\sin(km)}{m} (2g^m - 1) \right] \\ (\cos k - g) \cos \left[\sum_{m=1}^n \frac{\sin(km)}{m} (2g^m - 1) \right] + \sin k \sin \left[\sum_{m=1}^n \frac{\sin(km)}{m} (2g^m - 1) \right] \end{bmatrix}, \end{aligned}$$

As a result, the excitation probability correction reads

$$\begin{aligned} \delta p_k^{(n)} \approx & 2T \cos [\text{Si}(nk)] \quad (30) \\ & \times \int_0^\infty dg \sin \frac{k}{2} \left\{ (\cos k - g) \sin \left[\sum_{m=1}^n \frac{\sin(km)}{m} (2g^m - 1) \right] + \sin k \cos \left[\sum_{m=1}^n \frac{\sin(km)}{m} (2g^m - 1) \right] \right\} \\ & + \cos \frac{k}{2} \left\{ (\cos k - g) \cos \left[\sum_{m=1}^n \frac{\sin(km)}{m} (2g^m - 1) \right] + \sin k \sin \left[\sum_{m=1}^n \frac{\sin(km)}{m} (2g^m - 1) \right] \right\}. \quad (31) \end{aligned}$$

Next, we switch to the variable of $g \rightarrow 1 - g$, measuring the critical point from $g \approx 0$ to the ferromagnetic point $g = 1$, and restrict the integral as $\int_{-\infty}^1 dg \dots \approx \int_0^1$, as excitations are dominated by the small neighborhood of the critical point, $g = 0$ in the ferromagnetic phase. For convenience, we denote the argument of the cosines and sines by $\Phi(k, n, 1 - g) = 2 \sum_{m=1}^n \frac{\sin(km)}{m} g^m$, while the g independent part can be approximated by a similar integral approximation as in Eq. (19),

$$\sum_{m=1}^n \frac{\sin(km)}{m} \approx \int_{1/n}^1 dx \frac{\sin(nkx)}{x} = \text{Si}(nk) - \text{Si}(k). \quad (32)$$

Separating also the $\text{Si}(k)$ terms from the sines and cosines one obtains

$$\begin{aligned} \delta p_k^{(n)} \approx & 2T \cos [\text{Si}(nk)] \quad (33) \\ & \times \int_0^1 dg \sin \frac{k}{2} (\cos k - 1 + g) \cos [\text{Si}(k)] \sin [2\Phi(k, n, 1 - g) - \text{Si}(nk)] \\ & + \sin \frac{k}{2} (\cos k - 1 + g) \sin [\text{Si}(k)] \cos [2\Phi(k, n, 1 - g) - \text{Si}(nk)] + \sin \frac{k}{2} \sin k \cos [\text{Si}(k)] \cos [2\Phi(k, n, 1 - g) - \text{Si}(nk)] \\ & - \sin \frac{k}{2} \sin k \sin [\text{Si}(k)] \sin [2\Phi(k, n, 1 - g) - \text{Si}(nk)] + \cos \frac{k}{2} (\cos k - 1 + g) \cos [\text{Si}(k)] \cos [2\Phi(k, n, 1 - g) - \text{Si}(nk)] \\ & - \cos \frac{k}{2} (\cos k - 1 + g) \sin [\text{Si}(k)] \sin [2\Phi(k, n, 1 - g) - \text{Si}(nk)] + \cos \frac{k}{2} \sin k \sin [\text{Si}(k)] \cos [2\Phi(k, n, 1 - g) - \text{Si}(nk)] \\ & + \cos \frac{k}{2} \sin k \cos [\text{Si}(k)] \sin [2\Phi(k, n, 1 - g) - \text{Si}(nk)]. \end{aligned}$$

Now the key ingredient lies in the scaling behavior of g and k with respect to n after performing also the momentum integrals for the defect cumulants. For this, one needs to consider the general leading order behavior of the expansion

of $\Phi(n, k, 1 - g)$ with respect to both k and g ,

$$\Phi(n, k, 1 - g) = \sum_{l,j=0}^{\infty} \sum_{m=1}^n (-1)^l \frac{m^{2l}}{(2l+1)!} k^{2l+1} \binom{m}{j} g^j \sim \sum_{l,j=0}^{\infty} (nk)^{2l+1} (ng)^j. \quad (34)$$

As a result, $\Phi(n, k, 1 - g)$ simplifies to a bivariate function of nk and ng , denoted by $\tilde{\Phi}(nk, ng) \approx \Phi(n, k, 1 - g)$. As a result, integration of Eq. (33) with respect to both k and g with additional power of g^j and k^l in front of the sines and cosines will scale as n^{-2-l-j} . Therefore, for the leading behavior, one only needs to consider the lowest order expansion k and g . Exploiting the leading order behavior, $\text{Si}(k) \sim k$ one ends up with

$$\delta p_k \approx 2T \cos[\text{Si}(nk)] \int_0^1 dg g \cos[\tilde{\Phi}(nk, ng) - \text{Si}(nk)] + k \sin[\tilde{\Phi}(nk, ng) - \text{Si}(nk)]. \quad (35)$$

Quite interestingly, the excitation probabilities themselves do not acquire the same order with n explicitly, as the first term scales as n^{-2} after performing the integration with respect to g , while the second as kn^{-1} . However, as both terms involve additional functions depending only on nk , all cumulant integrals will scale as T/n^3 . As a result, the CD fast quench regime terminates when the above perturbative corrections reach the order of cumulants in the sudden limit, $T/n^3 \sim n^{-1}$, verifying the CD fast quench scale of $T_{\text{fast}}^{\text{CD}} \sim n^2$ holding for all cumulants.

Finally, the specific constant factor of the cumulants can be obtained by numerically integrating the double integrals of the cumulants of

$$\delta \kappa_1^{(n)}(T) \approx \frac{T}{n^3} \frac{L}{\pi} \int_0^\pi dk \int_{-\infty}^1 dg g \cos \left[2 \sum_{m=1}^n \frac{\sin(km)}{m} g^m - \text{Si}(nk) \right] + k \sin \left[2 \sum_{m=1}^n \frac{\sin(km)}{m} g^m - \text{Si}(nk) \right] \quad (36)$$

$$\equiv \frac{T}{n^3} \frac{L}{\pi} \int_0^\pi dk n^3 \delta p_k - 0.7T n^{-3},$$

$$\delta \kappa_2^{(n)}(T) \approx \frac{2T}{n^3} \frac{L}{\pi} \int_0^\pi dk n^3 \delta p_k (1 - 2p_k) \approx -1.5T n^{-3}, \quad (37)$$

$$\delta \kappa_3^{(n)}(T) \approx \frac{2T}{n^3} \frac{L}{\pi} \int_0^\pi dk n^3 \delta p_k (6p_k^2 - 6p_k + 1) \approx -3.55T n^{-3}. \quad (38)$$

CUMULANT EXPANSION FROM THE SLOW LIMIT

In this section, we show details of the analytical approximations for the transition probabilities in the independent TLS of the TFIM in the presence of CD. First, we realize that the results of Ref. [29],

$$q_k^{(n)} = -4 \dot{g}(t) \sum_{m=1}^n \sin(km) \frac{g^{2m} + g^L}{8g^{m+1}(1+g^L)} - \frac{\delta_{m,0}}{8g}, \quad (39)$$

can be expressed in more compact form. As the g^L terms will either dominate ($|g| > 1$) or disappear ($|g| < 1$), $q_k^{(n)}$ can be written as a geometrical sum,

$$q_k^{(n)} \approx \frac{i\dot{g}(t)}{4} \sum_{m=0}^{n-1} e^{ik} e^{ikm} g^{\text{sgn}(1-|g|)m} - e^{-ik} e^{-ikm} g^{\text{sgn}(1-|g|)m} \quad (40)$$

$$= -\dot{g} \begin{cases} \frac{\sin k - \sin(k(n+1))g^n + \sin(kn)g^{n+1}}{2(1+g^2-2g \cos k)}, & |g| < 1, \\ \frac{\sin k - \sin(k(n+1))g^{-n} + \sin(kn)g^{-(1+n)}}{2(1+g^2-2g \cos k)}, & |g| > 1. \end{cases} \quad (41)$$

For large enough expansion order, $n \gtrsim \sqrt{L}/10$ at momentum $k \gtrsim n^{-1}$ the numerator $\sin(k(n+1))g^n - \sin k - \sin(kn)g^{n+1}$ remains finite. To understand further, how the dynamics is affected, we concentrate on the avoided crossings that would form without CD around their approximate position, $g \approx 1 - k^2/2$. For $T \lesssim n^2$ and with the condition that the corresponding Landau-Zener (LZ) transition is of order $O(1)$, i.e., $k \ll T^{-1/2}$ implies that the CD matrix element scales as $q_k^{(n)} \sim (Tk^2)^{-1} \gg 1$. As a result, CD dominates the dynamics, ensuring adiabatic dynamics approximately. For $T \gg n^2$, however $Tk^2 \gg 1$ washing out the effect of CD and also leading to the suppression of LZ transitions, implying adiabaticity for the whole region of $k_n \gg n^{-1}$.

At the same time, for low momentum, $k = b/n$, $b \ll 1$ the numerator of $q_k^{(n)}$ can be expanded up to the leading, cubic order in k yielding for the off-diagonal CD term $q_k^{(n)} \sim (nk)^2/(kT)$. For slow quenches, $T = an^2$, $a \gtrsim 1$ the CD term scales as $q_k^{(n)} \sim b/(an)$. With the condition of $b \lesssim a^{-1/2}$, the matrix element is suppressed as $q_k^{(n)} \lesssim a^{-3/2}n^{-1}$, implying that the dynamics is insensitive to CD. The fast quench regime can also be addressed via the analysis of the LZ transition rates, provided that the driving time is not far away from the breakdown scale, $T = an^2$, $a \lesssim 1$. As a result, the CD term scales as $q_k^{(n)} \sim (nk)^2/(Tk) \sim b/(an) \ll 1$, thus leaving invariant this regime as well.

As a result, the cumulant generating function admits the form as reported in the main text with the LZ probabilities restricted below the momentum $k_n \sim n^{-1}$,

$$\log \tilde{P}^{(n)}(\theta; T) = \sum_{k < k_n} \log [1 + (e^{i\theta} - 1)p_k] = -L n_{\text{ex}} \sum_{p=1}^{\infty} \frac{(1 - e^{i\theta})^p}{p^{3/2}} \text{erf} \left(\frac{k_n \sqrt{p}}{2\sqrt{\pi} n_{\text{ex}}} \right),$$

where $n_{\text{ex}} = (8\pi^2 T)^{-1/2}$ is the average defect density without CD. This result shows that below the CD fast-quench threshold, defect statistics and all defect cumulants are insensitive to CD as for $k_n^2 T \gg 1$, i.e. $T \gg T_{\text{fast}}^{\text{CD}}$ the correction becomes exponentially close to the result of Ref. [49], $\text{erf} \left[\frac{k_n \sqrt{p}}{2\sqrt{\pi} n_{\text{ex}}} \right] \approx 1$. However, decreasing the driving time beyond the fast quench breakdown, the average extracted from Eq. (42) converges to a constant value,

$$\kappa_1^{(n)}(T) = -i\partial_{\theta} \log \tilde{P}^{(n)}(\theta; T) \Big|_{\theta=0} = L n_{\text{ex}} \text{erf} \left(\frac{k_n \sqrt{p}}{2\sqrt{\pi} n_{\text{ex}}} \right) \rightarrow \frac{k_n}{\pi} L. \quad (42)$$

This allows for fixing the constant factor in k_n by requiring that $n_{\text{ex}} \text{erf} \left[\frac{k_n \sqrt{p}}{2\sqrt{\pi} n_{\text{ex}}} \right] \approx 1.05/\pi n^{-1}$ leading to $k_n \propto 1.05 n^{-1}$ so that it reproduces the sudden quench limit.

Using this argument as an ansatz, the analytical structure of all cumulants can be captured approximatively around the CD fast quench breakdown providing a smooth function interpolating between the exact results in the fast and slow driving regimes. Similarly to the average, we restrict ourselves to the first-order expansion of Eq. (42) and fix the constant k_n so that the cumulants reach the exact CD fast quench values for $T \rightarrow 0$. As a result of the limiting form of the error function, $\text{erf}(x) = \frac{2}{\sqrt{\pi}}x + O(x^3)$ the approximation correction from the slow driving limit is given by

$$\kappa_q^{(n)}(T) \approx L \kappa_q^{\text{KZ}}(T) \text{erf} \left[\frac{\sqrt{\pi} \kappa_q^{(n)}(0)}{2\kappa_q^{\text{KZ}}(T)} \right] = L \kappa_q^{\text{KZ}}(T) \frac{2}{\sqrt{\pi}} \frac{\sqrt{\pi} \kappa_q^{(n)}(0)}{2\kappa_q^{\text{KZ}}(T)} + O(T^{3/2}) \approx \kappa_q^{(n)}(0), \quad (43)$$

where $\kappa_q^{\text{KZ}}(T)$ and $\kappa_q^{(n)}(0)$ denoting the q -th cumulant for the n -th order of expansion in the KZ scaling and sudden limits, respectively.

Note that this strategy replaces the approach of the $1/T$ expansion reported in Ref. [47]. In particular, without CD, the LZ formula only applies up to momentum $k \lesssim T^{-1/4}$. According to the results of Ref. [47], beyond the CD fast quench regime, $n^2 \ll T$, this implies a scale of $k \lesssim n^{-1/2}$. Thus, the KZ scaling regime beyond the CD fast quench threshold is completely governed by the LZ transitions.

UNIVERSALITY DEMONSTRATED BY APPROXIMATE METHODS IN THE LONG-RANGE KITAEV MODEL

In this section, we provide an approximate analytical treatment of the long range Kitaev models (LRKM). The momentum space representation of the LRKM provides an efficient platform to test the universality of the CD order scaling,

$$H(t) = -2g(t) \sum_{i=1}^L c_i^\dagger c_i - \sum_{i=1}^L \sum_{r=1}^{L/2} \left[j_{r,\alpha} c_i^\dagger c_{i+r} + d_{r,\beta} c_i^\dagger c_{i+r} + \text{h.c.} \right], \quad (44)$$

$$H = 2 \sum_{k>0} \hat{\psi}_k^\dagger [g(t) - j_\alpha(k)] \tau^z + d_\beta(k) \tau^x \hat{\psi}_k \equiv 2 \sum_{k>0} \hat{\psi}_k^\dagger H_k(t) \hat{\psi}_k, \quad (45)$$

$$j_{\alpha,r} = \mathcal{N}_\alpha r^{-\alpha} j_\alpha(k) = \mathcal{N}_\alpha^{-1} \sum_{r=1}^{L/2} r^{-\alpha} \cos(kr) \approx \text{Re} [\text{Li}_\alpha(e^{ik})], \quad (46)$$

$$d_{\beta,r} = \mathcal{N}_\beta r^{-\beta} d_\beta(k) = \mathcal{N}_\beta^{-1} \sum_{r=1}^{L/2} r^{-\beta} \sin(kr) \approx \text{Im} [\text{Li}_\beta(e^{ik})], \quad (47)$$

with $\mathcal{N}_\gamma = 2 \sum_{i=1}^{L/2} r^{-\gamma} \approx 2\zeta(\gamma)$. The exact CD term can conveniently be expressed as

$$H_{\text{CD}} = -\dot{g} \sum_{k>0} \frac{d_\beta(k)}{2 [d_\beta^2(k) + [g + j_\alpha(k)]]} \hat{\psi}_k^\dagger \tau_k^y \hat{\psi}_k = -\dot{g} \mathcal{N}_\beta \sum_{r=1}^{L/2} r^{-\beta} \sum_{k>0} \frac{\sin(kr)}{2 [d_\beta^2(k) + [g + j_\alpha(k)]]} \hat{\varphi}_k^\dagger r \tau_k^y \hat{\varphi}_k. \quad (48)$$

with $\hat{\varphi}_k = (c_k^\dagger, c_{-k})^T$. As the exact Krylov expansion of the LRKM cannot be obtained in a closed form, we develop an analytical ansatz starting from the exact results of the TFIM, but keeping the most important analytical properties of the LRKM, governing the leading order behavior of counterdiabatic critical dynamics. In particular, similar to the exact CD, all the Krylov expansion terms will depend only on k via the combination kr , while the overall order of magnitude is fixed by the energy gap denominator, similarly to the TFIM. To this end, we employ the approximation, in which the Krylov expansion is obtained independently for the different interaction ranges. As a result, the off-diagonal matrix element can be expanded in a similar way as for the TFIM

$$q_k^{(n)} = -\dot{g}(t) \sum_{r=1}^L \mathcal{N}_\beta^{-1} r^{-\beta} \sum_{m=1}^n \sum_{k'} \frac{\sin(k'r) \sin(k'rm)}{1 + g^2 - 2g \cos(k'r)} \sin(krm) \quad (49)$$

$$= -\dot{g} \sum_{r=1}^L \mathcal{N}_\beta^{-1} r^{-\beta-1} \sum_{m=1}^n \frac{g^{2m} + g^L}{2g^{m+1}(1 + g^L)} \sin(krm). \quad (50)$$

The expression in the first line can also be summed up, which will prove to be useful for studying the CD fast quench scale,

$$q_k^{(n)} \approx -\dot{g} \sum_{r=1}^L \mathcal{N}_\beta^{-1} r^{-\beta-1} \begin{cases} \frac{\sin k - \sin(k(n+1))g^n + \sin(kn)g^{n+1}}{[d_\beta(k) + (g - j_\alpha(k))]^2}, & |g| < 1, \\ \frac{\sin k - \sin(k(n+1))g^{-n} + \sin(kn)g^{-(1+n)}}{[d_\beta(k) + [g - j_\alpha(k)]]^2}, & |g| > 1. \end{cases} \quad (51)$$

where in the last step the exact energy gap of the k -th mode has been restored to get a more accurate approximation for the LRKM. The form in Eq. (49) provides a convenient framework to evaluate the sudden quench excitation probabilities via a similar integration as in Eq. (9). This leads to the following wave-function

$$e^{-i \int_0^T dt' q_k^{(n)}(t') \tau^y} \begin{pmatrix} 0 \\ 1 \end{pmatrix} = \begin{bmatrix} \cos \left[\int_0^T dt' q_k^{(n)}(t') \right] - i \sin \left[\int_0^T dt' q_k^{(n)}(t') \right] \tau^y \\ -\sin \left[\sum_r \mathcal{N}_\beta^{-1} r^{-\beta-1} [\text{Si}(n, rk) + (\pi - k)/2] \right] \\ \cos \left[\sum_r \mathcal{N}_\beta^{-1} r^{-\beta-1} [\text{Si}(n, rk) + (\pi - k)/2] \right] \end{bmatrix} \begin{pmatrix} 0 \\ 1 \end{pmatrix} \approx \begin{bmatrix} -\sin \left[\sum_r \mathcal{N}_\beta^{-1} r^{-\beta-1} \text{Si}(r\kappa) \right] \\ \cos \left[\sum_r \mathcal{N}_\beta^{-1} r^{-\beta-1} \text{Si}(r\kappa) \right] \end{bmatrix}. \quad (52)$$

Here the shorthand notations were used again $\text{Si}(z) = \int_0^z dt \frac{\sin t}{t}$, $\text{Si}(n, k) = \sum_{m=1}^n \frac{\sin(km)}{m}$ and with the new variable $\kappa = nk$. In the last step, we also neglected all pure k dependencies, as for large n they provide only subleading corrections for finite values of κ . From this, the excitation probability is given by projecting this state on the excited state of the k -th mode of the LRKM at $g = 0$ given by

$$|\text{ES}_k(0)\rangle = \frac{1}{\sqrt{d_\beta^2(k) + [j_\alpha(k) + \sqrt{j_\alpha^2(k) + d_\beta^2(k)}]^2}} \begin{bmatrix} -d_\beta(k) \\ j_\alpha(k) + \sqrt{j_\alpha^2(k) + d_\beta^2(k)} \end{bmatrix}. \quad (53)$$

The excitation probability thus reads

$$p_k \approx \frac{\left| d_\beta(k) \sin \left[\sum_r \mathcal{N}_\beta^{-1} r^{-\beta-1} \text{Si}(r\kappa) \right] + \cos \left[\sum_r \mathcal{N}_\beta^{-1} r^{-\beta-1} \text{Si}(r\kappa) \right] \left[j_\alpha(k) + \sqrt{j_\alpha^2(k) + d_\beta^2(k)} \right] \right|^2}{d_\beta^2(k) + \left[j_\alpha(k) + \sqrt{j_\alpha^2(k) + d_\beta^2(k)} \right]^2} \approx \cos^2 \left[\sum_r \mathcal{N}_\beta^{-1} r^{-\beta-1} \text{Si}(rnk) \right]. \quad (54)$$

This implies again that all cumulants are expected to scale inversely with the CD order for systems that can be decomposed to TLSs and where LZ transitions describe defect generation. Although the construction contained two

ansatz-motivated approximations, the essential physics was preserved throughout the derivations, namely that the interaction range and the CD order only enter the analysis via rk and nk . With this property at hand, it is a crucial consequence that the excitation probabilities are insensitive to the critical properties encoded in the final excited state as well.

Next, we deduce conclusions from Eq. (51) regarding the CD fast quench breakdown scale. A similar argument can be performed as for the TFIM, namely we concentrate on the properties of the avoided level crossings for large n and with small momentum, where $z = \min\{\beta, \alpha\} - 1$ for $\alpha < \min\{2, \beta\}$, $z = \beta - 1$ for $\alpha < \beta < 2$, and $z = 1$ otherwise.

To this end, let us consider the regime of momenta $k \gg 1/n$. The key observation is that the numerator of the approximative CD term remains finite, which also holds for the general set-up. For $T \lesssim n^{2z}$ either in the KZ or in the dynamical scaling regime [59] the condition for LZ transitions to have finite contributions is $T \ll k^{2z}$. Note that, due to the long-range behavior $1/(2z)$ only matches the KZ scaling power-law outside $\alpha < \min\{2, \beta\}$. Otherwise, it is given by $1/(2(\beta - 1)) < 1/(2z)$. As a result, the condition $T \ll k^{-2z}$ is a sharper bound than the one obtained by the KZ scaling exponent. Thus, the CD expansion dominates in this regime, implying adiabatic dynamics. In the opposite limit, $T \gtrsim n^{2z}$, the CD term vanishes and the LZ transitions are suppressed as well, $Tk^{2z} \gg 1$ both in the dynamical and in the KZ scaling case. As a result, modes above $k \gtrsim 1/n$ are driven adiabatically due to the fact that the CD term depends on the combination nk in the leading order.